Proceedings of the 39th IEEE
Conference on Decision and Control
Sydney, Australia • December, 2000

A Comparative Study on Subband Identification

Damian Marelli and Minyue Fu
dmarelli@ee.newcastle.edu.au and eemf@ee.newcastle.edu.au
Department of Electrical and Computer Engineering
University of Newcastle, N.S.W. 2308 Australia

Abstract. This paper reports some new study on the subband identification approach. We first provide a complete characterization for the subbands to be decoupled in the sense that different subband channels are statistically independent and the subband model is diagonal. We then apply this result to studying the performance of subband identification schemes based on recursive least-squares algorithms. We provide expressions for the computational cost, asymptotic residual error, and convergence rate. These expressions can be used to determine when the subband approach is advantageous over the full-band approach. A simulation example is given to demonstrate these advantages.

1 Introduction

The problem of linear system identification has been studied extensively, with many references available; see, e.g., [1, 2]. Algorithms based on LMS or least-squares are commonly used and their behaviors are well understood. However, a direct use of these algorithms is often found unsuitable for real-time applications such as speech echo cancellation and channel equalization where high order FIR models are typically required. For example, a typical room may have acoustic reverberations lasting 50ms. If speech signals are sampled at 20KHz rate, a 1000-tap FIR filter is required to model the reverberations. Implementing adaptive filters of such a high order requires very fast computation. Also, the convergence rate of very high order filters is typically very slow.

These difficulties has motivated a new line of research on system identification using subbands; see, e.g., [3, 4] and the references thereof. Roughly speaking, the subband approach divides the input and output signals into a number of subbands using two filter banks, and a model is identified for each subband channel. Sometimes the so-called "cross-filters" are used to model interferences between different subband channels [3]. These subband models are then combined to give a full-band model. A detailed description is given in Section 2. A lot of studies has been done to understand the performance of the subband approach. It is known that the subband approach leads to significant savings in computational time and convergence rate.

In this paper, we show some new study on the behavior of the subband identification approach. We consider a popular option of the subband approach where the subband channels are decoupled. The first problem we address is how to design the filter banks for the input and output signals so that the subband channels are decoupled in the sense that the signals in different channels are statistically independent and the subband model is diagonal. This property is important because in this case different channels can be identified separately. For critically sampled subbands, it is well-known that if the filter banks for the input and output signals are designed using ideal low-pass and band-pass filters, decoupling of the subband channels occurs. We show that this turns out to be the only possible design modulo channel permutations. Based on this, we give a complete characterization of all filter banks which achieve decoupling.

The next problem we analyze is the performance of the subband approach when a recursive least-squares identification algorithm is used for subbands. The motivation for this study stems from the fact most of the performance study done on subband identification is based on LMS algorithms; see [3, 4] and the references thereof. We give expressions for the computational cost, asymptotic residual error and convergence rate. These expressions can help us choose the number of subbands to achieve a good performance. It can also be seen from these expressions when the subband approach yields a superior performance in all the three aspects above. This is demonstrated via a simulation example, where the advantages of the subband identification are clearly demonstrated.

2 Subband Representation

Consider a single-input single-output linear time-invariant system with the following model:

$$
\begin{aligned}
w(z) &= g(z)u(z) \\
y(z) &= w(z) + v(z)
\end{aligned}
\tag{2.1}
$$

where $g(z)$ is the transfer function of the system, $u(z)$ is the input, $w(z)$ is the output, $v(z)$ is the measurement noise, and $y(z)$ is the received signal, all expressed in Z-transform. Their time-domain representations are to be denoted by $g(t), u(t), w(t)$ and $v(t)$, respectively.

The idea of subband identification is depicted in Figure 1. In this scheme, both the input and the received signals are split into subbands using two analysis filter banks $\mathbf{l}(z) = [l_0(z), l_1(z), \cdots, l_{D-1}(z)]^T$ and $\mathbf{h}(z) = [h_0(z), h_1(z), \cdots, l_{D-1}(z)]^T$ which are not necessarily the same. For simplicity reasons, we only consider the case of maximal decimation, i.e., the number of subband channels equals to the down-sampling rate. The subband identification is done via a transfer matrix model $\hat{G}(z)$ in the subband with the prediction of the subband model minimized in some way. Finally, the prediction error is converted back to the full-band using a synthesis filter bank $\mathbf{f}(z) = [f_0(z), f_1(z), \cdots, f_{D-1}(z)]^T$ to give an estimate of the noise, $\hat{v}(t)$.
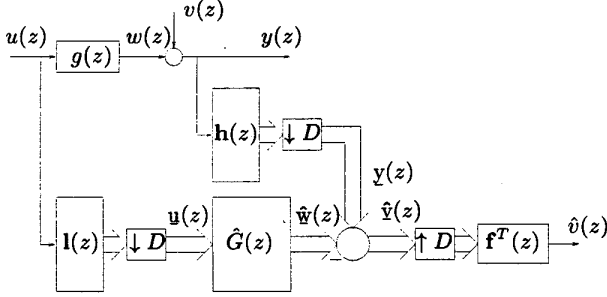

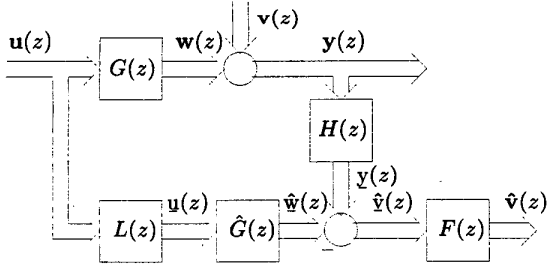**Figure 1:** Subband Identification Block Diagram

Figure 2: Polyphase Representation of Subband ID

An alternative representation of the subband identification scheme is the polyphase representation depicted in Figure 2. The relationship between the representations is standard [5] and is given below:

$$G(z) = \begin{bmatrix} g_0(z) & g_1(z) & \vdots & g_{D-1}(z) \\ z^{-1}g_{D-1}(z) & g_0(z) & \vdots & g_{D-2}(z) \\ & \cdots & & \\ z^{-1}g_1(z) & z^{-1}g_2(z) & \vdots & g_0(z) \end{bmatrix} \tag{2.2}$$

$$H(z) = \begin{bmatrix} h_{00}(z) & h_{01}(z) & \vdots & h_{0\check{D}}(z) \\ h_{10}(z) & h_{11}(z) & \vdots & h_{1\check{D}}(z) \\ & \cdots & & \\ h_{\check{D}0}(z) & h_{\check{D}1}(z) & \vdots & h_{\check{D}\check{D}}(z) \end{bmatrix} \tag{2.3}$$

where $\check{D} = D - 1$ and $g_i(z)$ is the ith polyphase component of $g(z)$, i.e.,

$$g(z) = \sum_{i=0}^{D-1} z^{-i} g_i(z^D) \tag{2.4}$$

A similar definition applies to $l_{ki}(z)$, $h_{ki}(z)$, etc. The matrix functions $L(z)$ and $F(z)$ are defined similarly to $H(z)$.

It is assumed throughout the paper that $H(z)$ and $L(z)$ are stable and invertible. The invertibility is required for the subband system to preserve all the information in the full-band.

It is straightforward to verify that the conditions for the subband to have the same representation as the full-band:

$$\hat{G}(z) = H(z)G(z)L^{-1}(z) \tag{2.5}$$

and

$$F(z)H(z) = z^{-d}I \tag{2.6}$$

where $d \geq 0$ is an integer to allow some delays in the noise estimate $\hat{v}$.

3 Decoupling of Subband

From the previous section, we understand that the subband model $\hat{G}(z)$ is required to satisfy (2.5) so that it is equivalent to $g(z)$ in the full-band. In general, the channels in the subband are coupled. This poses difficulties in identification of the subband system.

In this section, we seek the conditions under which the subband system is decoupled in the sense that the subband channels are statistically independent and the system model $\hat{G}(z)$ is diagonal. This case is of particular importance because different channels can be identified independently, leading to significant advantages in terms of computation cost, accuracy and convergence rate. These advantages will be analyzed in the next section.

We first rewrite $G(z)$ in (2.2) as follows:

$$G(z) = \sum_{i=0}^{D-1} g_i(z)E_i(z) \tag{3.1}$$

where

$$E_i(z) = \begin{bmatrix} 0 & I_{D-i} \\ z^{-1}I_i & 0 \end{bmatrix}, \quad i = 0, \cdots, D-1 \tag{3.2}$$

Then, (2.5) becomes

$$\hat{G}(z) = \sum_{i=0}^{D-1} g_i(z)\hat{E}_i(z) \tag{3.3}$$

where

$$\hat{E}_i(z) = H(z)E_i(z)L^{-1}(z) \tag{3.4}$$

In order for $\hat{G}(z)$ to become diagonal for all $g(z)$, or equivalently, for all $g_i(z), i = 0, \cdots, D-1$, it is necessary and sufficient that each $\hat{E}_i(z)$ must be diagonal. The following result gives the conditions under which $\hat{E}_i(z)$ are diagonal.

Theorem 1 *Consider the matrix functions $\hat{E}_i(z), i = 0, \cdots, D-1$, as defined in (3.4) with stable and invertible matrix functions $H(z)$ and $L(z)$. In order for all $\hat{E}_i(z), i = 0, \cdots, D-1$, to be diagonal, it is necessary and sufficient that*

$$\begin{array}{rcl} H(z) & = & \frac{1}{D}P(z)\Gamma_H(z)W\mathcal{D}(z^{-\frac{1}{D}}) \\ L(z) & = & \frac{1}{D}P(z)\Gamma_L(z)W\mathcal{D}(z^{-\frac{1}{D}}) \end{array} \tag{3.5}$$

where $\Gamma_H(z)$ and $\Gamma_L(z)$ are invertible diagonal transfer matrices, $P(z)$ is an arbitrary permutation matrix function, W is the so-called digital Fourier transform (DFT) matrix and is given by

$$W = \left[w^{ik}\right]_{i,k=0}^{D-1} \tag{3.6}$$

with $w = \exp(j2\pi/D)$ and

$$\mathcal{D}(z) = \text{diag}\{1, z^{-1}, \cdots, z^{-(D-1)}\} \tag{3.7}$$

In this case, $\hat{G}(z)$ and $g(z)$ are related by

$$\begin{array}{rcl} \hat{G}(z) & = & P(z)\Gamma_H(z)\text{diag}\{g_W^{(0)}(z), \cdots, g_W^{(D-1)}(z)\} \\ & & \cdot\Gamma_L^{-1}(z)P(z)^T \end{array} \tag{3.8}$$

and

$$\begin{array}{l} \left[\begin{array}{cccc} g_0(z) & g_1(z) & \cdots & g_{D-1}(z) \end{array}\right]^T \\ = \mathcal{D}^{-1}(z^{\frac{1}{M}})W\left(\Gamma_H^{-1}(z)P(z)^T\hat{G}(z)P(z)\Gamma_L(z)\right)_{\text{col}} \end{array} \tag{3.9}$$

where $(X)_{\text{col}}$ represents a column vector containing the diagonal elements of the matrix X, and

$$g_W^{(k)}(z) = \sum_{i=0}^{D-1} z^{-i/D}w^{-ik}g_i(z) \tag{3.10}$$

Proof: Obviously, any $H(z)$ and $L(z)$ can be expressed as in (3.5) with appropriate $\Gamma_H(z)$ and $\Gamma_L(z)$ which are not necessarily diagonal. Therefore, we need to prove that all $\hat{E}_i(z)$ are diagonal if and only if $\Gamma_H(z)$ and $\Gamma_L(z)$ are diagonal.

It is straightforward to verify that

$$\mathcal{D}(z^{\frac{1}{D}})E_i(z) = z^{-i/D}E_i(1)\mathcal{D}(z^{\frac{1}{D}}) \tag{3.11}$$

and

$$WE_i(1)W^{-1} = W^{(i)} \tag{3.12}$$

where

$$W^{(i)} = \text{diag}\{1, w^i, \cdots, w^{(D-1)i}\} \tag{3.13}$$

Hence,

$$\hat{E}_i(z) = z^{-i/D}P(z)\Gamma_H(z)W^{(i)}\Gamma_L^{-1}(z)P(z)^T \tag{3.14}$$

It is obvious that $\hat{E}_i(z)$ are diagonal if $\Gamma_H(z)$ and $\Gamma_L(z)$ are diagonal. It remains to prove the converse.

Denote by $\hat{e}_i^{(j)}(z)$, $w^{(j)}$ and $\gamma^{(j)}(z)$ the jth column of $\hat{E}_i(z)$, W and $\Gamma_L^{-1}(z)$, respectively. Also denote by $\Gamma^{(j)}(z)$ the diagonal matrix function with the kth diagonal element equal to the kth element of $\gamma^{(j)}(z)$. Also assume $P(z) = I$ for the moment. We then have

$$\hat{e}_i^{(j)}(z) = z^{-i/D}\Gamma_H(z)\Gamma^{(j)}(z)w^{(i)}$$

It follows that

$$\left[\begin{array}{cccc} \hat{e}_0^{(j)} & \hat{e}_1^{(j)} & \cdots & \hat{e}_{D-1}^{(j)} \end{array}\right] = \Gamma_H(z)\Gamma^{(j)}(z)W\mathcal{D}(z^{\frac{1}{D}}) \tag{3.15}$$

The fact that $\hat{E}_i(z)$ being diagonal implies that the left-hand side has all rows equals to zero except the jth row. This and the invertibility of $\Gamma_H(z)$ mean that all the elements in $\Gamma^j(z)$ except one must be zero so that the two sides of (3.15) can have the same rank. Further, the nonzero element in a different $\Gamma^j(z)$ must occur in a different row to assure that $\Gamma^{-1}(z)$ is nonsingular. Hence, $\Gamma^{-1}(z)$ is a diagonal matrix, modulo a z-dependent permutation matrix. Returning to (3.14), we also conclude that $\Gamma_H(z)$ must be a diagonal matrix, modulo the same permutation. Since the permutation matrix is considered in (3.5), $\Gamma_H(z)$ and $\Gamma_L(z)$ are diagonal. Finally, the verification of (3.8) and (3.9) is straightforward. ∎

Next, we investigate the conditions required for the subband channels to be statistically independent. To this end, we first consider the input signal to the subband. Denote by $\mathbf{u}(t)$ the subband input vector, i.e.,

$$\mathbf{u}(t) = [u(tD)\ u(tD+1)\ \cdots\ u(tD+D-1)]^T \tag{3.16}$$

Denote by $\phi_u(z)$ and $\Phi_{\mathbf{u}}(z)$ the spectral densities of $u(t)$ and $\mathbf{u}(t)$, respectively. Then, their relationship is given in the following lemma.

Lemma 2 *The spectral density $\Phi_{\mathbf{u}}(z)$ is given by*

$$\Phi_{\mathbf{u}}(z) = \sum_{i=0}^{D-1} \phi_{u,i}(z)E_i(z) \tag{3.17}$$

where $E_i(z)$ are given in (3.2) and $\phi_{u,i}(z)$ is the ith polyphase component of $\phi_u(z)$.

Proof: The autocorrelation matrix for $\mathbf{u}(t)$ reads

$$
\begin{aligned}
R(\tau) &= \mathcal{E}\{\mathbf{u}(t)\mathbf{u}^T(t+\tau)\} \\
&= [\mathcal{E}\{u(tD-i)u(tD+\tau D-j)\}]_{i,j=0}^{D-1} \\
&= [r_u(\tau D+j-i)]_{i,j=0}^{D-1}
\end{aligned}
$$

where $r_u(\tau)$ represents the autocorrelation function for $u(t)$. Then,

$$
\begin{aligned}
\Phi_{\mathbf{u}}(z) &= \left[\sum_{\tau=-\infty}^{\infty} r_u(\tau D+j-i)z^{-\tau}\right]_{i,j=0}^{D-1} \\
&= \sum_{i=0}^{D-1} \phi_{u,i}(z)E_i(z)
\end{aligned}
$$

∎

If we denote by $\phi_v(z)$ and $\Phi_{\mathbf{v}}(z)$ the spectral densities of $v(t)$ and $\mathbf{v}(t)$, respectively. Then, we also have

$$
\Phi_{\mathbf{v}}(z) = \sum_{i=0}^{D-1} \phi_{v,i}(z)E_i(z) \tag{3.18}
$$

Denote by $\Phi_{\underline{u}}(z)$ the spectral density matrix of $\underline{u}(t)$. We then have the following result.

Theorem 3 *A given invertible filter bank $H(z)$ is such that the spectral density matrix $\Phi_{\underline{u}}(z)$ is diagonal for all $\phi_u(z)$ if and only if*

$$
H(z) = \frac{1}{D}P(z)\Gamma_H(z)W\mathcal{D}(z^{\frac{1}{D}}) \tag{3.19}
$$

where $\Gamma_H(z)$ is a stable and invertible diagonal matrix function, and P, W and $D(z)$ are defined as in Theorem 1. In this case,

$$
\begin{aligned}
\Phi_{\underline{u}}(z) &= P(z)\Gamma_H(z)\text{diag}\left\{\sum_{i=0}^{D-1} z^{-i/D}w^{-i0}\phi_{u,i}(z),\right. \\
&\quad \left.\cdots,\sum_{i=0}^{D-1} z^{-i/D}w^{-i(D-1)}\phi_{u,i}(z)\right\} \\
&\quad \Gamma_H^{-1}(z^{-1})P(z)^T
\end{aligned}
$$

$$(3.20)$$

Proof: Note that

$$
\Phi_{\underline{u}}(z) = H(z)\sum_{i=0}^{D-1} \phi_{u,i}(z)E_i(z)H^*(z^{-1})
$$

where * denotes the Hermitian operation. We also note that $W^* = DW^{-1}$. The rest follows from Theorem 1 by taking $L^{-1}(z) = H^*(z^{-1})$. ∎

The decoupling conditions for the subband noise vector $\mathbf{v}(t)$ is similar.

We conclude this section by providing a remark on Theorems 1 and 3.

Remark 4 *It is assuring that the decoupling conditions for the subband model $\hat{G}(z)$, input spectrum density matrix, and noise spectrum density matrix are consistent. In fact, this property is easy to explain by comparing the two subband representations in Figures 1 and 2. If we consider the definition of the Alias Component Matrix [5] ($A_H(z)$ and $A_L(z)$), from (3.5), it follows that*

$$
\begin{aligned}
A_H^T(z^{\frac{1}{D}}) &= P(z)\Gamma_H(z) \\
A_L^T(z^{\frac{1}{D}}) &= P(z)\Gamma_L(z)
\end{aligned}
$$

The permutation matrix $P(z)$ allows subband channels to be formed using different arrangements of the portions of the unit circle; and the diagonal matrix functions $\Gamma_H(z)$ and $\Gamma_L(z)$ serve as shaping functions for the input and noise in the subbands. The significance of the results in Theorems 1 and 3 is of two-fold. First, it is shown that the above configuration for the subband filters is not only sufficient but also necessary. Secondly, mathematical relationships between the full-band and decoupled subband functions are revealed.

4 Comparative Study

The aim of this section is to compare the performances of the subband method with full-band method.

First, it should be noted that the ideal decoupling filters cannot be realized using rational functions, leaving alone FIR functions. In reality, FIR functions or IIR functions are used. This, of course, introduces approximation errors and residuals in off-diagonal terms in the subband model. To keep our analysis simple, we neglect these approximation errors.

As stated in remark 4, we can form a subband channel by combining several narrow-band channels. But this is not a practical choice because as we take narrower bands, the filter's impulse response becomes longer. We also want the filter coefficients to be real. So the optimal filter design is

$$
\begin{aligned}
h_m(e^{j\omega}) &= l_m(e^{j\omega}) = \frac{1}{D}f_m(e^{j\omega}) \tag{4.1} \\
&= \begin{cases} 1 & w \in \sigma_m \\ 0 & otherwise \end{cases} \quad m = 0,\cdots,D-1
\end{aligned}
$$

where $\sigma_m = [-\frac{m+1}{D}\pi, -\frac{m}{D}\pi] \cup [\frac{m}{D}\pi, \frac{m+1}{D}\pi]$.

Computational Cost. The computational cost depends on what recursive least squares (RLS) algorithm is used. In this analysis, we assume that the computational cost (measured in terms of the number of multiplications) in the full-band case is roughly equal to $9n$ per sample. This is in line with several fast RLS algorithms; see [6]. It is easy to see that the cost in the

subband case is $3l + 9n_s$ per (full-band) sample, where l is the tap size for each band-limited filter in the filter bank, and n_s is the average number of parameters in each subband. The choice for l should be $l = kD$, for some constant k. For large k and small D, this choice assures that the leakage power of the band-limited filter due to the finite tap size is independent of the number of subbands.

Asymptotic Residual Identification Error. One possible criterion for choosing the tap size for the model of each subband channel is to take

$$n_s = \frac{n + 2l}{D} = \frac{n}{D} + k \qquad (4.2)$$

This assures that the subband model has at least the same accuracy as the full-band model, if the approximation errors of the filter banks are negligible. In practice, this choice is often found to be too conservative, especially for high frequency bands where the signal and noise powers tend to be small.

Convergence Rate. Denote by $g_N(z)$ and $\hat{g}_N(z)$ the identified models of $g(z)$ using full-band and subband methods at sample N, respectively. Further define

$$S_{v/u} = \frac{1}{2\pi} \int_{-\pi}^{\pi} \frac{\phi_v(e^{j\omega})}{\phi_u(e^{j\omega})} d\omega$$

$$S_N = \frac{1}{2\pi} \int_{-\pi}^{\pi} |g(e^{j\omega}) - g_N(j\omega)|^2 d\omega$$

and $\hat{S}_N$ similarly. It is well-known [1] that

$$\mathcal{E}\{g_N(e^{j\omega})\} = g(e^{j\omega}) \qquad (4.3)$$

$$\lim_{N,n \to \infty} \mathcal{E}\{S_N\} = \frac{n}{N} S_{v/u}, \qquad (4.4)$$

provided that $u(t)$ and $v(t)$ are uncorrelated. The limit above is not needed if both $u(t)$ and $v(t)$ are also zero mean and white.

For the subband method, we have the following result on the convergence rate:

Theorem 5 *Suppose that $g(z)$ has order n or less and $u(t)$ and $v(t)$ are statistically independent and that the model for each subband channel, $\hat{g}_m(z)$, has the same order n_s. Then,*

$$\lim_{N,n_s \to \infty} \hat{S}_N = \frac{Dn_s}{N} S_{v/u}, \qquad (4.5)$$

Proof: From the definition of $\hat{S}_N$ and decoupling

property of the subbands, it follows that

$$\hat{S}_N = \sum_{m=0}^{D-1} \frac{1}{2\pi} \int_{\sigma_m} \left| g(e^{j\omega}) - \hat{g}_{m,N}(e^{jD\omega}) \right|^2 d\omega$$

$$= \frac{1}{D} \sum_{m=0}^{D-1} \frac{1}{2\pi} \int_{D\sigma_m} \left| g(e^{j\frac{\omega}{D}}) - \hat{g}_{m,N}(e^{j\omega}) \right|^2 d\omega$$

where $\hat{g}_{m,N}(z)$ is the identified model for the mth diagonal entry of $\hat{G}(z)$. Define

$$S_{v/u}^{(m)} = \frac{1}{2\pi} \int_{D\sigma_m} \frac{\phi_v(e^{j\omega})}{\phi_u(e^{j\omega})} d\omega, \qquad (4.6)$$

Also note that the number of samples for each subband is $1/D$ of that for the full-band. Now, we get

$$\mathcal{E}\{\hat{S}_N\} = \frac{1}{D} \sum_{m=0}^{D-1} \frac{n_s}{N/D} S_{v/u}^{(m)}$$

$$= \frac{Dn_s}{N} \left(\frac{1}{D} \sum_{m=0}^{D-1} S_{v/u}^{(m)} \right) = \frac{Dn_s}{N} S_{v/u}$$

∎

5 Simulation Results

In this section we demonstrate the performance of subband identification through two examples. The first one corresponds to a system with the impulse response shown in figure 3. For the fullband method, $n = 400$
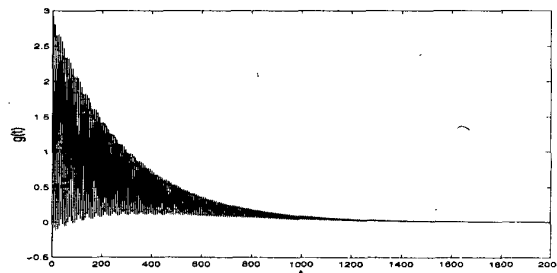

Figure 3: System's impulse response

is used. For the subband method, $D = 5$ and $k = 100$ are chosen. The same convergence rate can be achieved if we choose $n_s = 80$ for each channel. Unfortunately, this cannot guarantee that the asymptotic residual error in the subband method is comparable to the full-band method. We know from the impulse response in (3) that the main part of its energy is in the first two subbands, we can increase the number of parameters in these subbands by reducing the number of parameters in other bands. The effect of this shuffling on the convergence rate is difficult to assess but should be minimal

if $S_{v/u}^{(m)}$ defined in (4.6) does not vary much for different subbands.

In figure 4, the identification errors of both methods are plotted as a function of the number of samples processed. We can see that the convergence rate is ap-
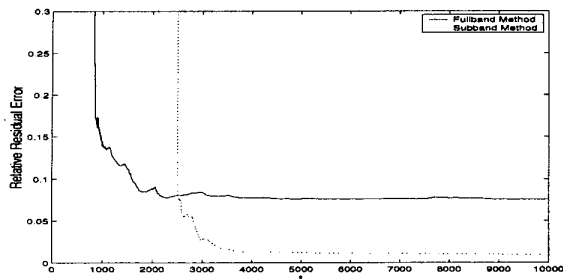

Figure 4: Residual error and convergence rate

proximately the same for the two methods and that the residual error is smaller for the subband method. It has to be noted that the subband method starts later because it has to accumulate a bigger number of data for the most important subbands. This is due to the shuffling of the parameters. It is easy to check that the subband method has only 62% of computation for the full-band method, which is the big advantage.

Figure 5 shows the normalized prediction error for $v(t)$, given by the two methods. It is clear that the subband method works better.

The second example involves estimation of the reverberation model in a room. A testing signal is sent out from a speaker and the reverberations are measured using a microphone. The settings for the full-band and subband methods are similar to the first example. The identification results are shown in Figure 6.
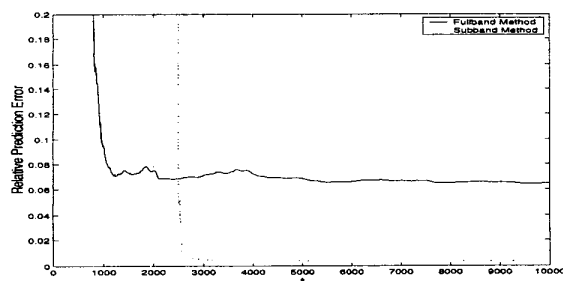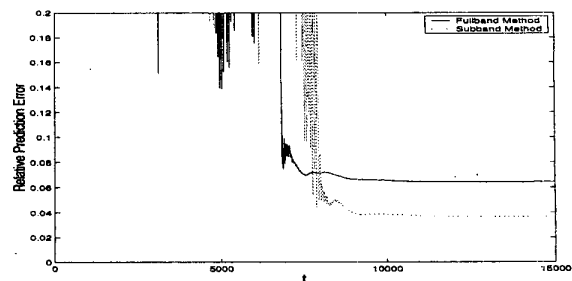

Figure 5: Prediction error for $v(t)$

Figure 6: Prediction error for the reverberation model

6 Conclusion

In this paper, we have studied the decoupling conditions for critically sampled subband identification. Based on these conditions, performance analysis has been done to understand the computational cost, asymptotic residual error and convergence rate of the subband method. It is clear that the subband method is suitable to applications where the full-band model is of very high order and computational cost is critical. In this case, the subband method offers compatible convergence rates but requires substantial less computation and gives less asymptotic residual errors. Simulation examples have been used to illustrate this point.

References

[1] L. Ljung, *System Identification: Theory for the User*, 2nd ed., Prentice Hall, 1999.

[2] M. L. Honing and D. G. Messerschmit, *Adaptive Filters: Structures, Algorithms, and Applications*, Boston: Kluwer, 1984.

[3] A. Gilloire and M. Vetterlli, "Adaptive filtering in subbands with critical sampling: analysis, experiments, and application to acoustic echo cancellation," *IEEE Trans. Signal Processing*, vol. 40, no. 8, pp. 1862-1875, August, 1992.

[4] Y. Lu and J. M. Morris, "Gabor expansion for adaptive echo cancellation," *IEEE Signal Processing Magzine*, pp. 68-80, March 1999.

[5] P. P. Vaidyanathan, *Multirate Systems and Filter Banks*, Prentice Hall, Englewood Cliifs, NJ, 1993.

[6] J. Proakis, *et. al.*, *Advanced Digital Signal Processing*, Macmillan, 1992.